SEMARAK ILMU PUBLISHING

Journal of Advanced Research in Fluid Mechanics and Thermal Sciences

Journal homepage:
https://semarakilmu.com.my/journals/index.php/fluid_mechanics_thermal_sciences/index
ISSN: 2289-7879

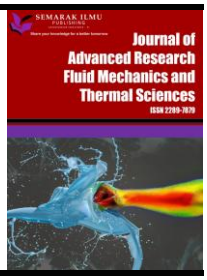

Transesterification of Waste Cooking Oil Utilizing Potassium Doped Empty Fruit Bunches Ash Heterogeneous Catalyst

Haifa Izz Awatif Hairol Jefri[1], Norshahidatul Akmar Mohd Shohaimi[1,2,*], Siti Fadhilah Ibrahim[1], Nurasmat Mohd Shukri[3], Naimat Abimbola Eleburuike[4]

[1] Faculty of Applied Sciences, Universiti Teknologi MARA Pahang, Bandar Tun Razak, 26400 Jengka, Pahang, Malaysia
[2] Advanced Biomaterials and Carbon Development Research Group, Faculty of Applied Sciences, Universiti Teknologi MARA, 40450 Shah Alam, Selangor, Malaysia
[3] School of Health Sciences, Universiti Sains Malaysia, Health Campus, 16150 Kubang Kerian, Kelantan, Malaysia
[4] Al-Hikmah University, Adeta Road, Ilorin, 240281, Kwara, Nigeria

ARTICLE INFO

Article history:
Received 14 October 2024
Received in revised form 12 January 2025
Accepted 21 January 2025
Available online 20 February 2025

Keywords:
EFBA; biodiesel; WCO; metal oxides

ABSTRACT

The growing demand for fossil fuels has prompted the exploration of alternative sustainable energy sources like biodiesel, renowned for its renewable nature and eco-friendliness. Empty fruit bunch ash (EFBA) has attracted significant interest due to its composition of various metal oxides, making it a promising option for creating high-performance heterogeneous catalysts. The synthesis of EFBA involves the co-precipitation method, where it is activated by KOH catalyst, denoted to as K/EFBA. This method enables the metal oxides in EFBA to bond with KOH, forming a catalyst with mixed metal oxides that enhances catalytic efficiency and prevents the loss of active sites. The K/EFBA catalyst exhibits a robust basicity of 2215.05 µmol/g, with more active sites resulting from the interaction of metal oxides, capable of converting waste cooking oil (WCO) into fatty acid methyl esters (FAME). Optimal conditions for transesterification of WCO, including a 7 wt% catalyst loading, 45 minutes reaction time, and a 12:1 methanol to oil ratio, yielded a biodiesel output of 70.51%. Gas chromatography-mass spectrometry (GCMS) analysis identified six peaks corresponding to different FAME groups, such as lauric acid methyl ester, myristic acid methyl ester, palmitic acid methyl ester, oleic acid methyl ester, and linoleic acid methyl ester. These results underscore the potential of the K/EFBA catalyst in converting WCO into biodiesel.

1. Introduction

Fossil fuels significantly contribute to global energy demand, but they are non-renewable and costly. Furthermore, burning fossil fuels generates greenhouse gases (GHGs) and particulate matter, exacerbating some of the world's most critical environmental issues. Consequently, researchers have increasingly focused on alternative renewable energy sources to reduce reliance on fossil fuels. Among these, biodiesel stands out as the most practical option. The term "bio" refers to its natural

* *Corresponding author.*
E-mail address: akmarshohaimi@uitm.edu.my

https://doi.org/10.37934/arfmts.127.2.133147

origin, while "diesel" denotes its use as a fuel, as suggested by its name [1]. Biodiesel or FAME is considered an ideal alternative to petroleum fuel due to its sulfur-free composition, high oxygen content, sustainability, and low hydrocarbon emissions [2]. Biodiesel can be produced from vegetable oils, animal fats, and waste products. Edible oil feedstocks include sunflower oil, soybean oil, palm oil, and coconut oil [3]. Non-edible feedstocks include oils from castor bean seeds, neem, rubber trees, rice bran, tobacco seeds, animal fats, waste cooking oils, and microalgal lipids. The primary method for biodiesel production is transesterification, a reversible catalytic reaction that occurs under mild conditions, reducing costs and increasing yield. This reaction is accelerated by the presence of an acid or base catalyst [4]. Essentially, the process involves exchanging the ester group with the OH group from alcohols like methanol or ethanol. Through three reversible stages, triglycerides are converted into diglycerides, monoglycerides, and glycerol, producing alkyl esters at each stage. Oil triglycerides react with alcohol in a 1:3 stoichiometric ratio with the aid of a catalyst. This process requires an excess amount of alcohol beyond the stoichiometric ratio to push the reaction towards equilibrium [5,6].

As noted by Welter *et al.,* [7], vegetable oils were the predominant feedstock in the biodiesel industry in 2023. However, their utilization has diminished due to increased costs and concerns about resource scarcity. Consequently, low-quality alternatives like WCO have emerged as potential substitutes [8]. WCO, sourced from edible vegetable oils used in cooking or frying in restaurants and households, possesses high levels of free fatty acids (FFA) and moisture content. Despite this, WCO is capable of yielding biodiesel at rates exceeding 90%. For instance, Mohadesi *et al.,* [9] achieved an impressive yield of 98.26% using WCO with a 1.16 wt% catalyst concentration and a reaction temperature of 62.4°C within 30-120 seconds. Similarly, Sabzi *et al.,* [10] investigated WCO using Metal-Organic Frameworks (MOFs) as catalysts and attained conversions of up to 98.8% at 145°C with a 24.18% catalyst amount over 7.5 hours. These findings highlight WCO as a promising feedstock due to its cost-effectiveness, widespread availability, eco-friendliness, and capacity to yield biodiesel at high rates. Additionally, utilizing WCO helps mitigate environmental concerns associated with its disposal into sewage pipelines.

Catalysts are employed to accelerate reaction rates. Homogeneous basic catalysts like NaOH and KOH, and homogeneous acid catalysts such as H_2SO_4, HCl, and H_3PO_4, are favored for their rapid reaction rates and high yields. However, separating these catalysts from the liquid product is challenging, rendering them non-reusable and prone to issues like saponification, emulsification, and high corrosiveness [11]. In contrast, heterogeneous catalysts offer several advantages, including broader selectivity, adaptability to high FFAs, and water tolerance. Heterogeneous catalysts are non-toxic, less complex, and more stable [12]. Examples of basic heterogeneous catalysts include CaO, KOH/Al_2O_3, KOH/NaY, Al_2O_3/KI, and alumina/silica supported K_2CO_3 Heterogeneous acid catalysts encompass heteropoly acids, zeolites, and modified transition metals supported on materials like silica, alumina, zirconium, and molybdenum. These catalysts exhibit greater stability, environmental friendliness, ease of separation, and reusability.

EFBA is readily available, particularly in Malaysia and Indonesia, as these nations are the primary producers of palm oil, contributing to around 85%-90% of global production. Approximately 23%-25% of EFBA is generated for every ton of EFB processed, potentially leading to a surplus of waste if not efficiently utilized [13]. EFBA, a type of biomass, contains various metal oxides such as KO_2, Al_2O_3, CaO, Fe_2O_3, and others, making it suitable for catalytic applications. EFBA presents an opportunity for sustainable utilization as a heterogeneous catalyst. In a study by Biswal and Sarkar [14] fly ash mixed with NaOH-catalyzed soybean oil, achieving a 97.8% conversion rate with a fly ash to NaOH mass ratio of 1:3. The presence of aluminosilicates and rare earth metals in fly ash enhances the structural, textural, and morphological properties of the catalyst. Oloyede *et al.,* [15] investigated

biodiesel production using calcined ash catalyst derived from agricultural residues, reporting successful conversion rates of 80-99.8%, with up to five recycling cycles yielding appreciable biodiesel. Therefore, basic heterogeneous catalysts derived from ash materials have the potential to produce high-yield biodiesel while maintaining high catalytic activity and stable structural properties. Ash materials have thus emerged as a viable option for renewable energy resources in the biodiesel industry due to their availability, lower cost, and capacity to mitigate environmental issues.

The objective of this research is to create a novel heterogeneous catalyst through the co-precipitation method, doping ash materials with KOH catalyst. A comprehensive discussion based on characterization findings is presented. The study explores the application of EFBA mixed with KOH material by utilizing WCO as feedstock to assess catalyst performance. The evaluation includes optimizing parameters such as catalyst loading, reaction time, reaction temperature, and methanol to oil molar ratio.

2. Methodology

2.1 Material and Feedstock

The feedstock of WCO was obtained from household area in Bandar Pusat Jengka, Pahang and the EFBA obtained from FTJ Bio Power Sdn. Bhd. Potassium hydroxide (KOH, 99%), n-hexane (purity > 99%), methanol (purity > 99%), methyl heptadecanoate (purity > 99%), sodium hydroxide (NaOH, 99%), phenolphthalein ($C_{20}H_{14}O_4$, 99%), hydrochloric acid (HCl, purity > 32%). All reagents were directly purchased with analytical grade and used without further purification. The WCO obtained undergoes filtration process to remove the solid particles and other impurities. After the WCO has been filtered, it was heated at 120°C while stirring for 2 h to remove water content and any impurities. Then, the pre-treated WCO was stored in a clean container. The physicochemical properties of WCO were analysed and presented in Table 1.

Table 1
Physical properties of WCO

Properties	WCO
Acid value (wt%)	2.48
FFA value (wt%)	1.24
Saponification value (mg KOH g^{-1})	109.74
Molecular weight ($gmol^{-1}$)	1533.85
Moisture content (%)	0.04

2.2 Catalyst Preparation

The alkaline activation process of EFBA with KOH involved mixing 20 g of EFBA with 44.56 mL of 2 M KOH and heating the mixture to 90°C until dry. Once the reaction mixture had completely dried, it was placed in an oven for 12 hours at 110°C. The treated EFBA was then ground into a smooth powder, resulting in the final product known as K/EFBA. Similarly, for the calcined sample, the same procedure was repeated followed by calcination, where the material was heated in a furnace at 600°C, resulting in the final product known as K/EFBA600.

2.3 Catalyst Characterization

Characterization of the catalyst was conducted to evaluate its physicochemical properties and morphological structure. Thermal decomposition was analyzed using a TGA-DTG curve with a TGA-

Pyris 2012 and a GSA7-Perkin Elmer thermal gas detector, which is equipped with differential thermogravimetry (DTG). Fourier transform infrared spectroscopy (FTIR) was performed using a Perkin Elmer Spectrum TM 100 FTIR instrument to identify active species on the catalyst, employing the universal Attenuated Total Reflectance (ATR) method for compound identification. Morphological and elemental composition analyses were carried out using a TESCAN VEGA3 scanning electron microscope (SEM) equipped with energy-dispersive X-ray spectroscopy (EDX). X-ray diffraction (XRD) analysis was used to determine the internal structure, bulk phase, and crystalline phase composition, utilizing a LabX XRD-6100 PANalytical powder X-ray diffractometer with Cu Kα radiation (30 kV, 15 mA). Mineral and elemental species of the catalysts were identified using standards from the Joint Committee on Powder Diffraction Standards (JCPDS). Pore size distribution and specific surface area were analyzed using the BET model with a Micromeritics ASAP 2010 instrument. The Barrett-Joyner-Halenda (BJH) method was applied for pore size distribution, while the BET method was used for specific surface area determination. The density of active sites and basic distribution of the catalyst were determined using carbon dioxide-temperature programmed desorption (CO_2-TPD) analysis with a Thermo Finnigan TPDRO 1100 series, measuring CO_2 gas desorption with a Thermocouple detector (TCD). Elemental composition and leaching spots on the solid sample were measured using an XRF instrument model S2 PUMA series in a helium atmosphere.

2.4 Biodiesel Analysis

The FAME composition in biodiesel samples was determined using a Gas Chromatography – Mass Spectrometry (GC-MS) model (GC-7890A, Agilent Technologies). Both the injector and detector temperatures were set to 240°C. Helium was employed as the gas carrier with a flow rate of 19.2 mL/min. The column temperature was maintained at 150°C with a ramping rate of 15°C/min for warm-up. The instrument's column temperature was then set to 300°C for startup, with a ramping rate of 7°C/min. A 1 µL sample was injected into the GC inlet port. From the obtained chromatogram, the peak area of FAME in biodiesel was identified and compared with the peak area of the internal standard (methyl heptadecanoate). Utilizing the equation below, the percentage of biodiesel yield from the transesterification reaction could be calculated:

$$Biodiesel\ (\%), d = (Weight\ of\ biodiesel\ collected\ (g)/10\ g\ of\ WCO)\ \times 100 \quad (1)$$

Due to the presence of unreacted oil, glycerol and other impurities, the ester content can be calculated using GC-MS analysis. By using Agilent method EN14103, ester content can be calculated using the formula below:

$$Ester\ content\ (\%), c = (TA - AEI/AEI)\ \times (CEI\ \times VEI/m)\ \times 100 \quad (2)$$

where c is ester content FAME, m is mass of the sample for GC-MS analysis, TA is total area of FAME, AEI is area of internal standard, CEI is concentration of internal standard solution (mg/mL) and VEI is volume of methyl heptadecanoate solution (mL).

$$Mass\ of\ biodiesel, Y = (c/100)\ \times m \quad (3)$$

where c is from the previous calculation from GC-MS analysis and m is mass of biodiesel collected after transesterification reaction.

$$Biodiesel\ yield\ (\%), B = (Y/10\ g\ of\ WCO)\ \times 100 \quad (4)$$

3. Results

3.1 Catalyst Characterization

TGA was employed to assess the thermal stability of K/EFBA. As depicted in Figure 1, a slight weight loss of 3.20% at temperatures around 30-50°C is attributed to the evaporation of absorbed water. Between 50-100°C, a 7.90% weight loss is due to the total elimination of water molecules associated with K/EFBA. At 600-700°C, there is a 4.90% weight loss resulting from the dihydroxylation of OH molecules [16]. From 700-900°C, an 8.20% weight loss is observed, caused by deposit formation and ash aggregation [17,18]. Furthermore, the TG curve indicates that thermal decomposition of EFBA can still occur, and 900°C is insufficient to achieve complete combustion [19,20].

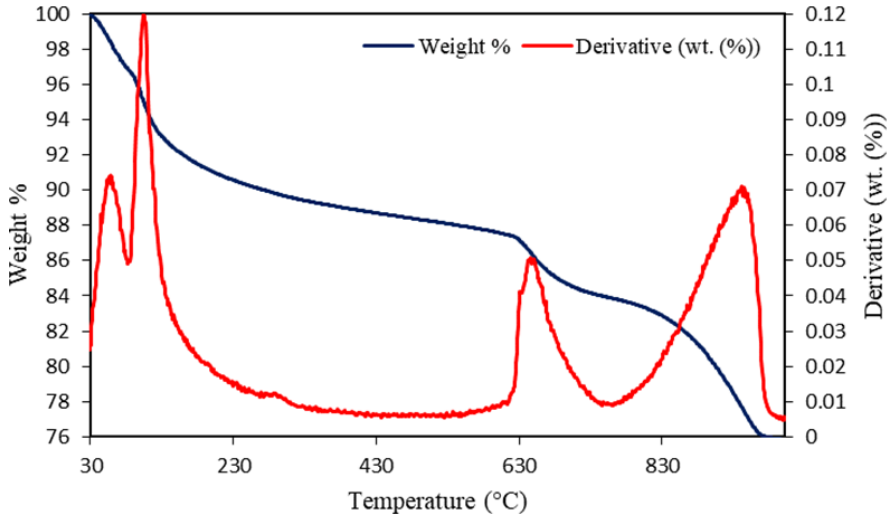

Fig. 1. TGA analysis of K/EFBA

Figure 2 displays the XRD patterns of K/EFBA and K/EFBA600. The highest peak for K/EFBA is at 2θ = 28.68°, corresponding to $CaSi_2$ with a tetragonal structure (JCPDS No. 00-019-0251). Additional peaks at 2θ = 29.82° and 2θ = 32.29° correspond to FeS (JCPDS No. 03-065-1894) and Mg (JCPDS No. 00-001-1141), respectively. A peak at 2θ = 40.79° indicates the formation of KCl with a cubic structure (JCPDS No. 00-001-0790), supported by another peak at 2θ = 50.19°. The presence of KCl is consistent with findings by Romero *et al.,* [21], who reported that KCl (sylvite) typically appears in ash compounds.

For K/EFBA600, only two peaks are observed: one at 2θ = 29.82° for FeS (JCPDS No. 03-065-1894) and another at 2θ = 40.79° for KCl (JCPDS No. 00-001-0790). After calcination, the peaks for FeS and Mg disappear, and the intensity of the KCl and $CaSi_2$ peaks is reduced. This disappearance suggests structural degradation of the particles at high temperatures [22]. Therefore, K/EFBA demonstrates better catalytic abilities compared to K/EFBA600, as it retains more active sites on the catalyst surface.

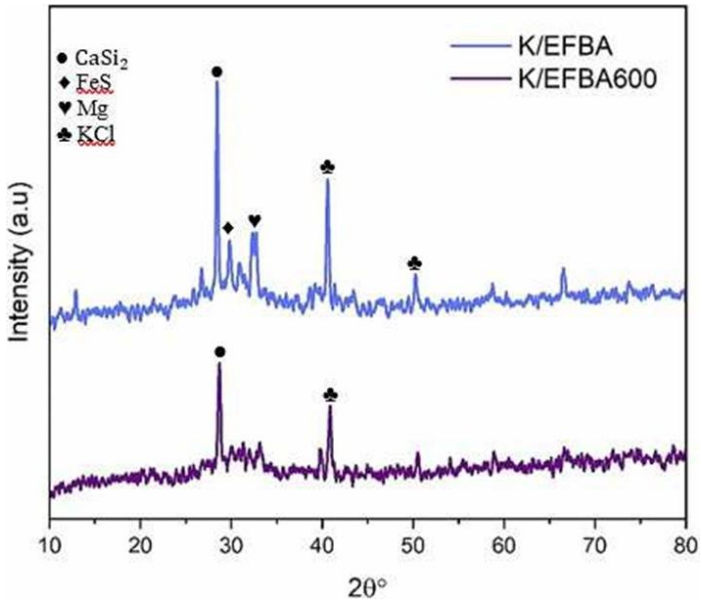

Fig. 2. XRD analysis for K/EFBA and K/EFBA600

Figure 3 presents SEM micrographs of K/EFBA and K/EFBA600 samples, both exhibiting irregular plate structures. Specifically, the K/EFBA micrograph in Figure 3(a) shows coarse particles formed by the aggregation of smaller particles, along with small agglomerate particles [21,23]. In contrast, the K/EFBA600 micrograph in Figure 3(b) reveals a densely agglomerated structure, consistent with data reported by Namkung *et al.,* [24]. This dense agglomeration is attributed to the high calcination temperature, which increases the tendency for agglomeration.

The EDX spectrum in Figure 3(c) and Figure 3(d) indicates the presence of various metals in the catalyst, including K, Ca, Si, Mg, Al, Fe, S, C, and O. The significant presence of O suggests the formation of metal oxides in the K/EFBA structure, enhancing the catalyst's basicity [25]. Both catalysts show a high amount of K, which significantly enhances their basicity and catalytic activity. However, the presence of alkali and alkaline earth metals reduces the ash melting temperature, increasing particle stickiness and agglomeration properties. K is the most abundant alkaline earth metal in EFBA, contributes to this effect [24]. The addition of KOH to EFBA further promotes agglomeration in the catalyst structure. Other metal oxides present in EFBA have minimal effect due to their low concentrations. The XRF analysis in Table 2 confirms the high percentages of K_2O and other basic metal oxides in K/EFBA, explaining the high basicity of the catalysts [26].

Both fresh and spent K/EFBA catalysts were chemically analyzed using XRF, as shown in Table 2, to determine the elemental composition and the leaching of active sites. K_2O is the most abundant element in the catalyst, followed by SiO_2, CaO, and Cl. The study revealed a significant leaching of K_2O from the catalyst surface. This observation aligns with the BET data, which show that the spent catalyst has a higher surface area than the fresh catalyst due to the leaching of initially deposited K on the surface [27]. According to Noiroj *et al.,* [28], this leaching occurs due to the chemical instability of the catalysts during the reaction.

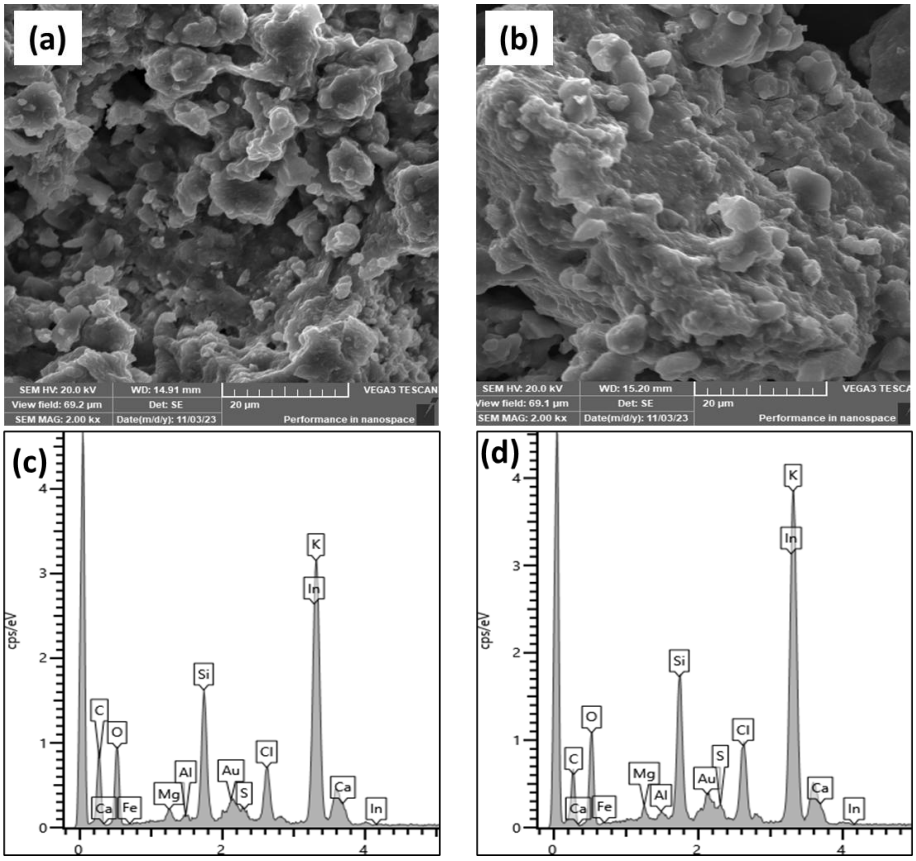

Fig. 3. SEM images (a) K/EFBA and (b) K/EFBA600 with 2Kx magnification and EDX spectrums (c) K/EFBA and (d) K/EFBA600

Table 2
XRF analysis of fresh and spent of K/EFBA

Component	Composition (wt%)	
	K/EFBA	Spent K/EFBA
K_2O	55.80	46.30
SiO_2	19.90	23.90
CaO	7.11	10.90
Cl	6.10	5.39
Fe_2O_3	3.21	4.52
SO_3	3.08	2.62

Brunauer-Emmett-Teller (BET) analysis was conducted to determine the surface area and pore structure of the catalysts. Figure 4 shows the isotherm graph for fresh and spent K/EFBA and K/EFBA600. According to IUPAC classifications, the nitrogen adsorption isotherms for both fresh and spent K/EFBA and K/EFBA600 are Type IV with hysteresis loops of Type H3, indicating mesoporous structures characterized by aggregates of plate-like particles forming slit-shaped pores [19,26,29]. Additionally, all catalyst samples have an average pore diameter between 20 and 40 nm, confirming their mesoporous nature [16].

Table 3 presents the BET surface area, total pore volume, and average pore diameter, calculated using the Barrett, Joyner, and Halenda (BJH) method. It was observed that K/EFBA has a lower surface area compared to K/EFBA600, although both catalysts show an increase in surface area after use. According to Ghasemi and Dehkordi [27], the smaller surface area of K/EFBA compared to K/EFBA600 is due to KOH loading, which covers the porous surface of the catalyst. The decrease in surface area is also attributed to sintering, which results in particle enlargement and crystallization [22]. The

higher surface area of the spent catalysts compared to the fresh ones is due to the leaching of active species such as K_2O (as shown in Table 2), which increases the catalyst's surface area.

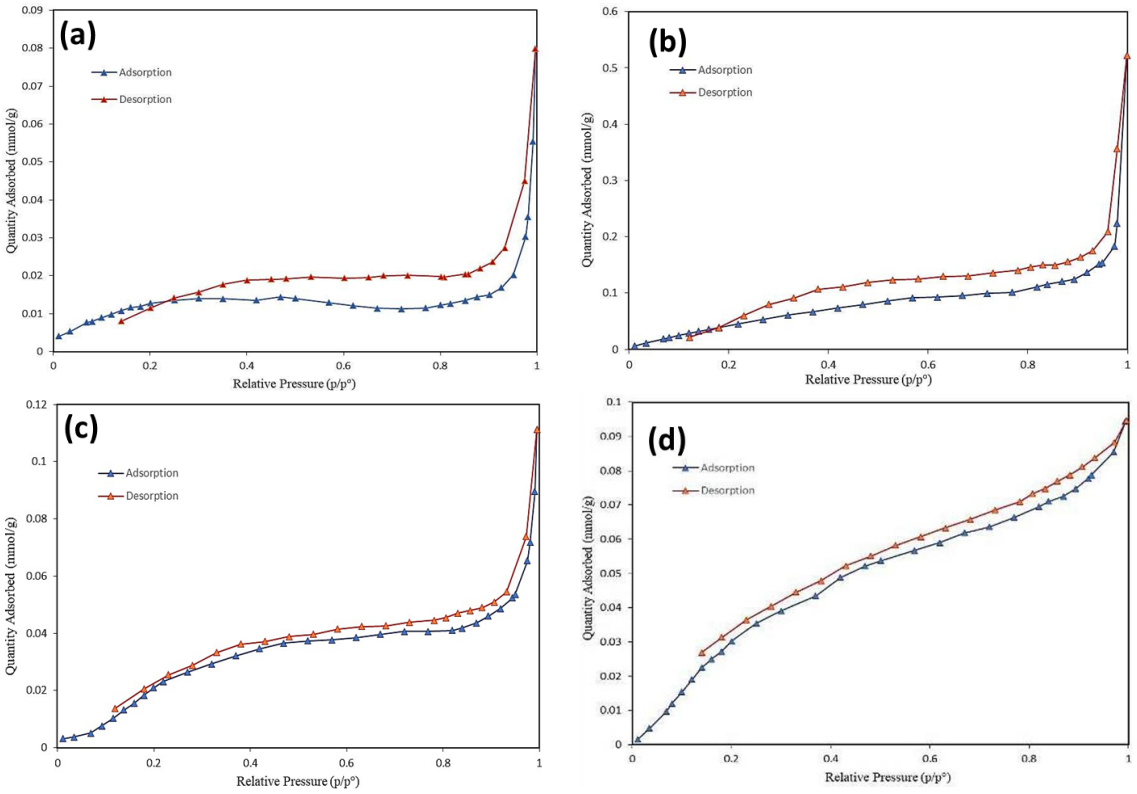

Fig. 4. BET isotherm graph for (a) fresh K/EFBA, (b) spent K/EFBA, (c) fresh K/EFBA600 and (d) spent K/EFBA600

Table 3
Physical properties of catalyst based on BET analysis

Catalyst	S_{BET} (m^2/g)	Total pore volume (cm/g)	Average pore diameter (nm)
Fresh K/EFBA	1.23	0.0026	34.20
Spent K/EFBA	5.55	0.0173	38.35
Fresh K/EFBA600	4.52	0.0033	20.04
Spent K/EFBA600	5.89	0.0035	21.23

Figure 5 showed the CO_2-TPD analysis was used to assess the basicity of K/EFBA and K/EFBA600, which is crucial for enhancing catalytic activity during the transesterification of WCO. The results indicate that both catalysts exhibit a broad desorption peak in the strong basicity region (above 550°C), suggesting significant CO_2 adsorption by electron donors with O_2^- ions, similar to findings by Abdullah *et al.,* [30]. In the weak basicity region (below 250°C), K/EFBA shows a minor peak, while K/EFBA600 displays a sharp peak. Despite this, the basic density of K/EFBA is higher, at 2215.05 µmol/g, compared to K/EFBA600's 1587.59 µmol/g, due to metal-metal interactions from transition metal oxides [31]. These results suggest that K/EFBA is more effective in converting WCO to biodiesel.

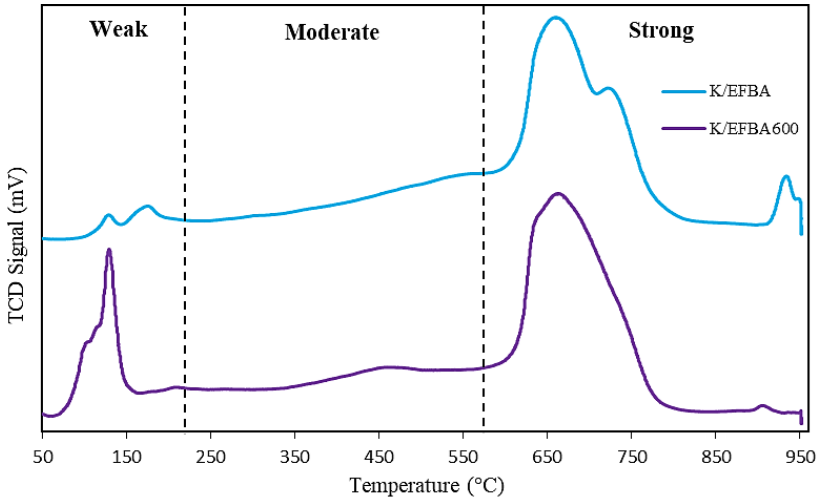

Fig. 5. CO_2-TPD of of K/EFBA and K/EFBA600

Figure 6 presents the FTIR spectra for both fresh and spent K/EFBA and K/EFBA600. The broad peaks at 3295.93 cm^{-1} and 3282.66 cm^{-1} are attributed to the OH band, further supported by the OH stretching observed at 683.38 cm^{-1} and 667.79 cm−1, indicating water molecules adsorbed onto the catalyst surface [26]. Figure 6(a) and Figure 6(b) illustrates that the fresh catalysts, K/EFBA and K/EFBA600, exhibit lower water content on their surfaces compared to the spent catalysts, suggesting that the fresh catalysts demonstrate higher catalytic activity, as corroborated by BET and XRF analysis results. Additionally, peaks at 1033.51 cm^{-1} and 1034.09 cm^{-1} in the fresh catalysts' spectra are attributed to the alternating SiO and AlO bonds and the catalyst's bending plane [19,26]. The peaks at 1407.92 cm^{-1} and 1403.52 cm^{-1} are due to the CH bending vibrations in the CH_2 groups of cellulose [32]. The spectra for the spent catalysts, K/EFBA and K/EFBA600, show similarities to the fresh catalysts but with significantly increased peak intensities due to catalyst degradation during the reaction and washing processes [19]. Furthermore, Figure 6(b) indicates the loss of several peaks in the spent K/EFBA600 compared to the fresh K/EFBA600, attributed to the calcination process, which decomposes organic compounds into carbon dioxide and water [26]. This loss of functional groups is due to the dehydration and deoxygenation of lignocellulosic materials (cellulose, hemicellulose, and lignin), resulting in the reduction of aliphatic structures and the formation of aromatic compounds [33].

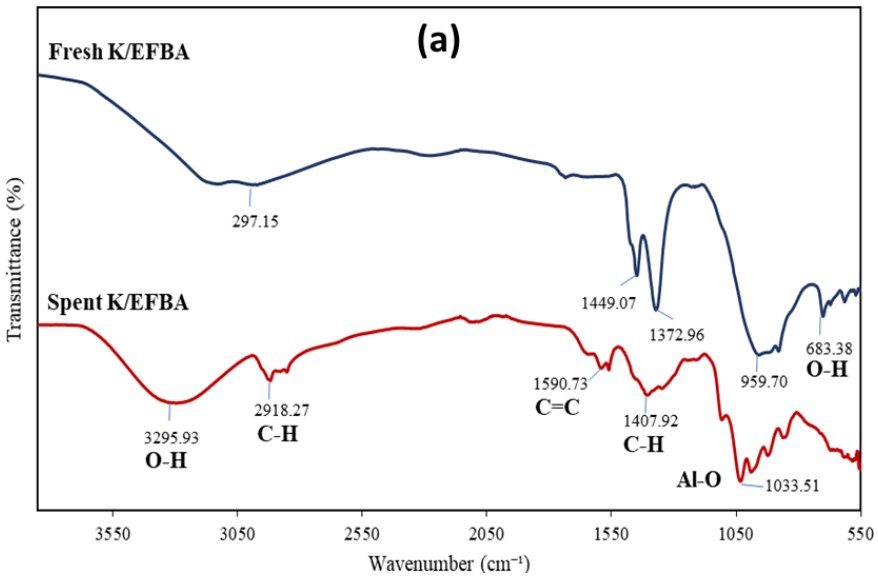

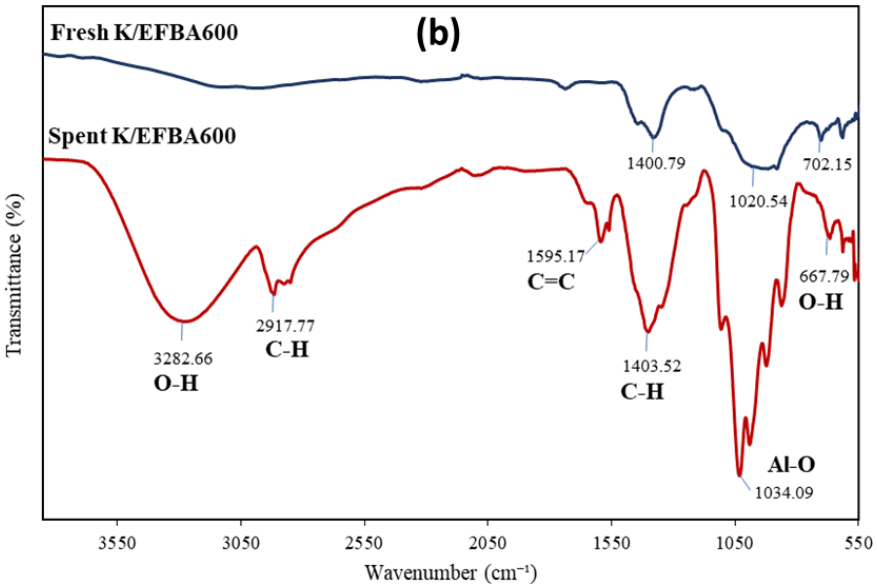

Fig. 6. FTIR analysis of fresh and spent catalyst of (a) K/EFBA and (b) K/EFBA600

3.2 Transesterification of WCO

The transesterification was conducted using a K/EFBA catalyst. Figure 7(a) displays the FTIR analysis for FAME, WCO, and glycerol. The FTIR analysis for FAME and WCO revealed similar functional groups, such as the carbonyl group, indicating a successful conversion to FAME due to their chemical similarity [34]. The absorption peaks for FAME around 2923.02 cm^{-1} and 2922.37 cm^{-1} were attributed to the C-H asymmetric and symmetrical stretching vibrations of the saturated C-C bond, while the significant peaks around 1742.26 cm^{-1} and 1744.13 cm^{-1} were assigned to the C=O group of the triglycerides. Peaks observed in the range of 1000–1300 cm^{-1} were attributed to the C–O stretching vibrations of the ester group. Additionally, peaks located at 722.06 cm^{-1} and 721.20 cm^{-1} were attributed to the overlapping of the CH_2 and the out-of-plane vibration CH wag of cis-di-substituted olefins, suggesting that the product consisted of long-chain FAME [35,36]. The spectra of glycerol were also similar to those of FAME and WCO; however, glycerol exhibited an additional peak at 3307 cm^{-1}, which was assigned to OH stretching [37,38]. The presence of carboxylic acids, ketones, and aldehydes groups further confirmed the successful conversion to FAME, correlating with GC-MS yield results [39].

The composition of FAME was determined using GC-MS analysis. WCO biodiesel was catalyzed under optimized conditions using K/EFBA. Figure 7(b) displays the GC-MS analysis of WCO biodiesel, revealing seven peaks for the compounds present in the biodiesel, with six peaks corresponding to methyl ester groups and one peak corresponding to internal standard. Table 4 showed details composition of methyl esters in WCO biodiesel: lauric acid methyl ester (0.43%), myristic acid methyl ester (1.18%), palmitic acid methyl ester (17.59%), oleic acid methyl ester (22.68%), and linoleic acid methyl ester (7.03%).

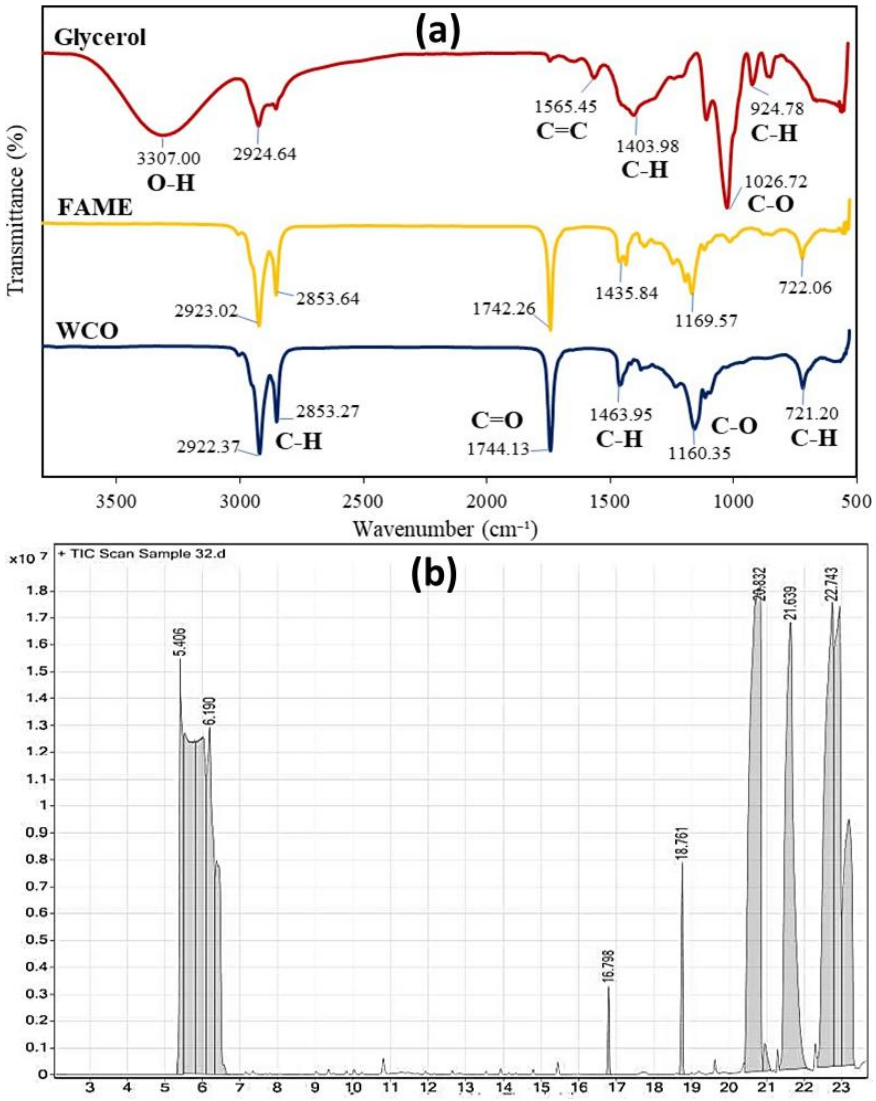

Fig. 7. (a) FTIR and (b) GC-MS chromatogram catalysed by K/EFBA

Table 4
Compound listed in GC-MS analysis for WCO biodiesel

Retention time (min)	Compound name	Composition (%)
16.798	Lauric acid methyl ester	0.43
18.761	Myristic acid methyl ester	1.18
20.832	Palmitic acid methyl ester	17.59
21.639	Methyl heptadecanoate	13.12
22.743	Oleic acid methyl ester	13.27
22.944	Oleic acid methyl ester	9.41
23.190	Linoleic acid methyl ester	7.03

3.3 Optimization Parameter

The optimization of the transesterification reaction assessed the efficacy of K/EFBA using the Langmuir-Hinshelwood-Hougen-Watson (LHHW) kinetic model. The parameters studied included the effects of methanol-to-oil molar ratio, reaction time, and catalyst loading. The investigation explored different effect on methanol-to-oil ratios, which are 9:1, 12:1, 15:1, and 18:1. In Figure 8(a), it is observed that the biodiesel yield percentage at a 9:1 ratio stood at 41.79% FAME, which increased to 58.82% at a 12:1 ratio. According to Farid *et al.,* [40], insufficient methanol might impede FAME

conversion, requiring excess methanol to push the reaction towards equilibrium [35,40]. Therefore, at a 12:1 ratio, there was sufficient methanol for FAME conversion. However, elevating the ratio to 15:1 and 18:1 led to diminished biodiesel yields of 46.5% and 34.93%, respectively. As indicated by Maniam *et al.,* [41], transesterification reactions are fundamentally reversible. Hence, further increasing the molar ratio of methanol may reverse the reaction, reducing yield percentages. Thus, the optimal methanol-to-oil molar ratio was determined at 12:1, yielding 58.82% FAME.

Figure 8(b) illustrates the effect of reaction time on transesterification (30, 45, 60, 75, and 90 mins). Biodiesel yield increased from 30 to 45 minutes (51.43% to 58.82%) before gradually declining at 60 minutes (56.79%), 75 minutes (39.9%), and 90 minutes (36%). Optimal reaction time is crucial as short durations lead to poor feedstock and methanol mixing, while prolonged times may force equilibrium reversal [42,43]. Thus, 45 minutes was deemed the optimal reaction time.

In Figure 8(c), the effect of catalyst loading (5 wt%, 7 wt%, 10 wt%, 13 wt%, and 15 wt%) was examined. A 1 wt% K/EFBA catalyst yielded up to 67.63% conversion, increasing to 70.51% at 2 wt%. This suggests that 2 wt% contains sufficient active sites for triglyceride conversion. However, further increases in loading (3 wt%, 4 wt%, and 5 wt%) reduced conversion to 66.34%, 66.13%, and 58.82%, respectively. This reduction is attributed to increased particle density leading to catalyst particle agglomeration, hindering stirring and methoxide ion mass transfer into the triglyceride layer, thereby decreasing methyl ester conversion [26,44]. Thus, the optimal catalyst loading was determined to be 7 wt%, yielding 70.51% biodiesel.

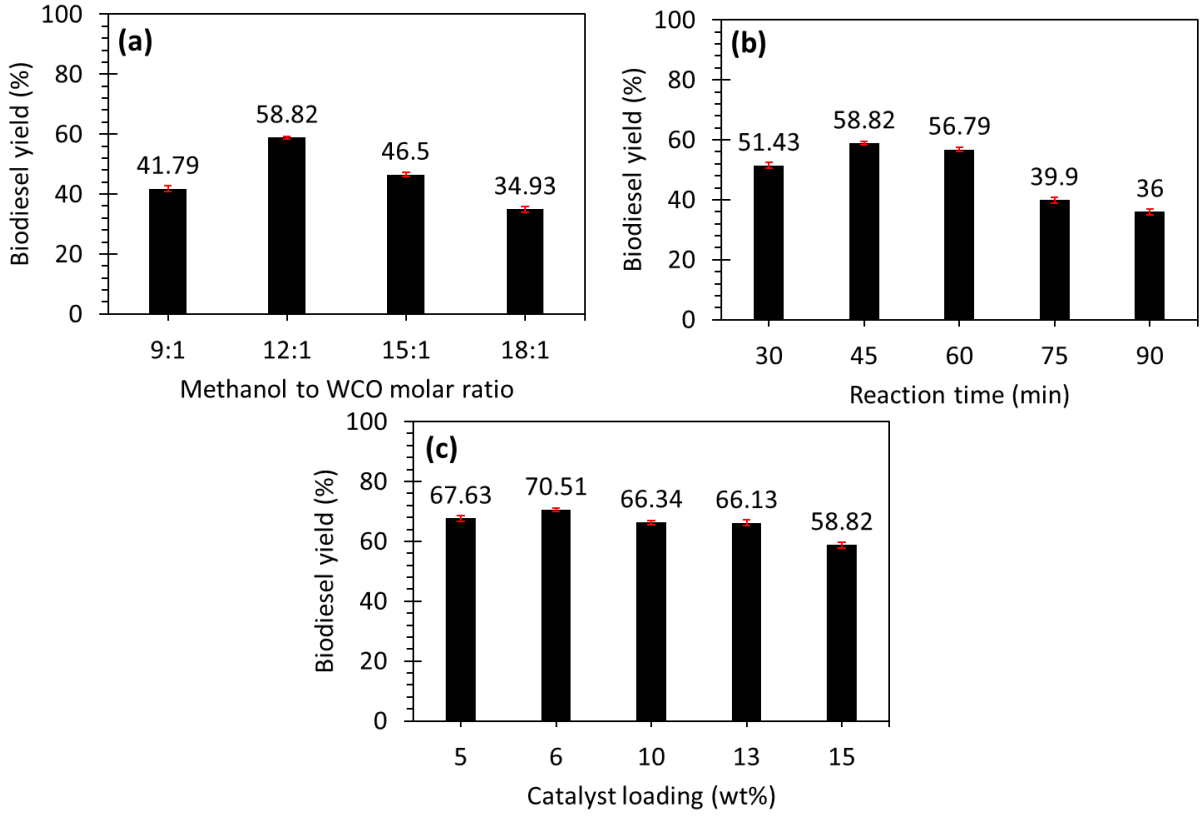

Fig. 8. Effect of optimization parameter on transesterification of WCO (a) Methanol to oil ratio (15 wt% of catalyst loading, 45 min reaction time and 65°C reaction temperature), (b) Reaction time (12:1 methanol to oil ratio, 15 wt% of catalyst loading and 65℃ reaction temperature), and (c) Catalyst loading (12:1 methanol to oil ratio, 45 min reaction time and 65°C reaction temperature)

4. Conclusions

The activation of EFBA as a heterogeneous basic catalyst using KOH via the co-precipitation method demonstrated outstanding catalytic performance, showcasing a strong basicity of 2215.05 µmol/g compared to K/EFBA calcined at 600°C. This activation led to a remarkable conversion rate of up to 70.15% FAME under conditions of 7 wt% catalyst loading, 45 minutes of reaction time, and a 12:1 methanol to oil ratio. Analysis of the resulting biodiesel via GC-MS identified six peaks corresponding to lauric acid methyl ester, myristic acid methyl ester, palmitic acid methyl ester, oleic acid methyl ester, and linoleic acid methyl ester. The comprehensive characterization of the catalyst suggests that K/EFBA holds promise for further applications in biodiesel production, making it a suitable and efficient heterogeneous catalyst for transesterification reactions to produce a sustainable clean energy [45].

Acknowledgement

Authors acknowledge the Ministry of Higher Education (MOHE) for funding under the Fundamental Research Grant Scheme (FRGS) (FRGS/1/2021/STG05/UITM/02/4).

References

[1] Gupta, Naveen Kumar. "Biodiesel production from waste cooking oil using mechanical stirring and ultrasonic cavitation method." In *IOP Conference Series: Materials Science and Engineering*, vol. 1116, no. 1, p. 012067. IOP Publishing, 2021. https://doi.org/10.1088/1757-899X/1116/1/012067

[2] Wang, Xiao-Man, Ya-Nan Zeng, Yu-Ran Wang, Fu-Ping Wang, Yi-Tong Wang, Jun-Guo Li, Rui Ji et al. "A novel strategy for efficient biodiesel production: Optimization, prediction, and mechanism." *Renewable Energy* 207 (2023): 385-397. https://doi.org/10.1016/j.renene.2023.03.027

[3] Mohiddin, Mohd Nurfirdaus Bin, Yie Hua Tan, Yee Xuan Seow, Jibrail Kansedo, N. M. Mubarak, Mohammad Omar Abdullah, Yen San Chan, and Mohammad Khalid. "Evaluation on feedstock, technologies, catalyst and reactor for sustainable biodiesel production: A review." *Journal of Industrial and Engineering Chemistry* 98 (2021): 60-81. https://doi.org/10.1016/j.jiec.2021.03.036

[4] Suzihaque, M. U. H., Habsah Alwi, Ummi Kalthum Ibrahim, Sureena Abdullah, and Normah Haron. "Biodiesel production from waste cooking oil: A brief review." *Materials Today: Proceedings* 63 (2022): S490-S495. https://doi.org/10.1016/j.matpr.2022.04.527

[5] Pydimalla, Madhuri, Sadia Husaini, Akshara Kadire, and Raj Kumar Verma. "Sustainable biodiesel: A comprehensive review on feedstock, production methods, applications, challenges and opportunities." *Materials Today: Proceedings* 92 (2023): 458-464. https://doi.org/10.1016/j.matpr.2023.03.593

[6] Nurfitri, Irma, Gaanty Pragas Maniam, Noor Hindryawati, Mashitah M. Yusoff, and Shangeetha Ganesan. "Potential of feedstock and catalysts from waste in biodiesel preparation: a review." *Energy Conversion and Management* 74 (2013): 395-402. https://doi.org/10.1016/j.enconman.2013.04.042

[7] Welter, Rosilene Andrea, Harrson Silva Santana, Lucimara Gaziola de la Torre, Mark C. Barnes, Osvaldir Pereira Taranto, and Michael Oelgemöller. "Biodiesel Production by Heterogeneous Catalysis and Eco-friendly Routes." *ChemBioEng Reviews* 10, no. 2 (2023): 86-111. https://doi.org/10.1002/cben.202200062

[8] Weldeslase, Mebrhit Gebreyohanes, Natei Ermias Benti, Mekonnen Abebayehu Desta, and Yedilfana Setarge Mekonnen. "Maximizing biodiesel production from waste cooking oil with lime-based zinc-doped CaO using response surface methodology." *Scientific Reports* 13, no. 1 (2023): 4430. https://doi.org/10.1038/s41598-023-30961-w

[9] Mohadesi, Majid, Babak Aghel, Mahmoud Maleki, and Ahmadreza Ansari. "Study of the transesterification of waste cooking oil for the production of biodiesel in a microreactor pilot: The effect of acetone as the co-solvent." *Fuel* 273 (2020): 117736. https://doi.org/10.1016/j.fuel.2020.117736

[10] Sabzi, Mazaher, Majid Baghdadi, Arash Aliasghar, and Maryam Pazoki. "Synthesis of MIL-68 (Al) Catalyst and Optimization of Green Biodiesel Production from Waste Cooking Oil." *Catalysis Letters* 154 (2024): 4885-4904. https://doi.org/10.1007/s10562-024-04659-1

[11] Chin, L. H., B. H. Hameed, and A. L. Ahmad. "Process optimization for biodiesel production from waste cooking palm oil (Elaeis guineensis) using response surface methodology." *Energy & Fuels* 23, no. 2 (2009): 1040-1044. https://doi.org/10.1021/ef8007954

[12] Maneerung, Thawatchai, Sibudjing Kawi, Yanjun Dai, and Chi-Hwa Wang. "Sustainable biodiesel production via transesterification of waste cooking oil by using CaO catalysts prepared from chicken manure." *Energy Conversion and Management* 123 (2016): 487-497. https://doi.org/10.1016/j.enconman.2016.06.071

[13] Hantoko, Dwi, Mi Yan, Bayu Prabowo, and Herri Susanto. "Preparation of empty fruit bunch as a feedstock for gasification process by employing hydrothermal treatment." *Energy Procedia* 152 (2018): 1003-1008. https://doi.org/10.1016/j.egypro.2018.09.107

[14] Biswal, Debraj, and Dipanwita Sarkar. "Biofuels From Macroalgae: A Sustainable Alternative to Conventional Energy Resources." In *Biomass and Bioenergy Solutions for Climate Change Mitigation and Sustainability*, pp. 148-169. IGI Global, 2023. https://doi.org/10.4018/978-1-6684-5269-1.ch009

[15] Oloyede, Christopher Tunji, Simeon Olatayo Jekayinfa, Abass Olanrewaju Alade, Oyetola Ogunkunle, Nsikak-Abasi Ubohon Otung, and Opeyeolu Timothy Laseinde. "Exploration of agricultural residue ash as a solid green heterogeneous base catalyst for biodiesel production." *Engineering Reports* 5, no. 1 (2023): e12585. https://doi.org/10.1002/eng2.12585

[16] Nolhakim, Muhammad Amirrul Hakim Lokman, Norshahidatul Akmar Mohd Shohaimi, Mohd Lokman Ibrahim, Wan Nur Aini Wan Mokhtar, and Ahmad Zamani Ab Halim. "Transesterification of waste cooking oil utilizing heterogeneous K_2CO_3/Al_2O_3 and KOH/Al_2O_3 catalysts." *Malaysian Journal of Chemistry* 23, no. 2 (2021): 74-83. https://doi.org/10.55373/mjchem.v23i2.1000

[17] Nyakuma, Bemgba Bevan, Anwar Johari, Arshad Ahmad, and Tuan Amran Tuan Abdullah. "Thermogravimetric analysis of the fuel properties of empty fruit bunch briquettes." *Jurnal Teknologi* 67, no. 3 (2014). T https://doi.org/10.11113/jt.v67.2768

[18] Madhiyanon, T., P. Sathitruangsak, S. Sungworagarn, S. Fukuda, and S. Tia. "Ash and deposit characteristics from oil-palm empty-fruit-bunch (EFB) firing with kaolin additive in a pilot-scale grate-fired combustor." *Fuel Processing Technology* 115 (2013): 182-191. https://doi.org/10.1016/j.fuproc.2013.05.018

[19] Okoye, Patrick U., Song Wang, Lanlan Xu, Sanxi Li, Jianye Wang, and Linnan Zhang. "Promotional effect of calcination temperature on structural evolution, basicity, and activity of oil palm empty fruit bunch derived catalyst for glycerol carbonate synthesis." *Energy Conversion and Management* 179 (2019): 192-200. https://doi.org/10.1016/j.enconman.2018.10.013

[20] Chala, Girma T., Ying P. Lim, Shaharin A. Sulaiman, and Chin L. Liew. "Thermogravimetric analysis of empty fruit bunch." In *MATEC Web of Conferences*, vol. 225, p. 02002. EDP Sciences, 2018. https://doi.org/10.1051/matecconf/201822502002

[21] Romero, Esperanza, Mar Quirantes, and Rogelio Nogales. "Characterization of biomass ashes produced at different temperatures from olive-oil-industry and greenhouse vegetable wastes." *Fuel* 208 (2017): 1-9. https://doi.org/10.1016/j.fuel.2017.06.133

[22] Mohamed, Mohamad Azuwa, Wan Norharyati Wan Salleh, Juhana Jaafar, Mohamad Saufi Rosmi, Zul Adlan Mohd Hir, Muhazri Abd Mutalib, Ahmad Fauzi Ismail, and Masaki Tanemura. "Carbon as amorphous shell and interstitial dopant in mesoporous rutile TiO_2: Bio-template assisted sol-gel synthesis and photocatalytic activity." *Applied Surface Science* 393 (2017): 46-59. https://doi.org/10.1016/j.apsusc.2016.09.145

[23] Vadery, Vinu, Binitha N. Narayanan, Resmi M. Ramakrishnan, Sudha Kochiyil Cherikkallinmel, Sankaran Sugunan, Divya P. Narayanan, and Sreenikesh Sasidharan. "Room temperature production of jatropha biodiesel over coconut husk ash." *Energy* 70 (2014): 588-594. https://doi.org/10.1016/j.energy.2014.04.045

[24] Namkung, Hueon, Young-Joo Lee, Ju-Hyoung Park, Gyu-Seob Song, Jong Won Choi, Joeng-Geun Kim, Se-Joon Park, Joo Chang Park, Hyung-Taek Kim, and Young-Chan Choi. "Influence of herbaceous biomass ash pre-treated by alkali metal leaching on the agglomeration/sintering and corrosion behaviors." *Energy* 187 (2019): 115950. https://doi.org/10.1016/j.energy.2019.115950

[25] Chin, L. H., B. H. Hameed, and A. L. Ahmad. "Process optimization for biodiesel production from waste cooking palm oil (Elaeis guineensis) using response surface methodology." *Energy & Fuels* 23, no. 2 (2009): 1040-1044. https://doi.org/10.1021/ef8007954

[26] Boey, Peng-Lim, Shangeetha Ganesan, Sze-Xooi Lim, Sau-Lai Lim, Gaanty Pragas Maniam, and Melati Khairuddean. "Utilization of BA (boiler ash) as catalyst for transesterification of palm olein." *Energy* 36, no. 10 (2011): 5791-5796. https://doi.org/10.1016/j.energy.2011.09.005

[27] Ghasemi, Mohammad, and Asghar Molaei Dehkordi. "Transesterification of waste cooking oil to biodiesel using KOH/γ-Al2O3 catalyst in a new two-impinging-jets reactor." *Industrial & Engineering Chemistry Research* 53, no. 31 (2014): 12238-12248. https://doi.org/10.1021/ie403408r

[28] Noiroj, Krisada, Pisitpong Intarapong, Apanee Luengnaruemitchai, and Samai Jai-In. "A comparative study of KOH/Al_2O_3 and KOH/NaY catalysts for biodiesel production via transesterification from palm oil." *Renewable Energy* 34, no. 4 (2009): 1145-1150. https://doi.org/10.1016/j.renene.2008.06.015

[29] Abdullah, Rose Fadzilah, Umer Rashid, Yun Hin Taufiq-Yap, Mohd Lokman Ibrahim, Chawalit Ngamcharussrivichai, and Muhammad Azam. "Synthesis of bifunctional nanocatalyst from waste palm kernel shell and its application for biodiesel production." *RSC Advances* 10, no. 45 (2020): 27183-27193. https://doi.org/10.1039/D0RA04306K

[30] Abdullah, Rose Fadzilah, Umer Rashid, Balkis Hazmi, Mohd Lokman Ibrahim, Toshiki Tsubota, and Fahad A. Alharthi. "Potential heterogeneous nano-catalyst via integrating hydrothermal carbonization for biodiesel production using waste cooking oil." *Chemosphere* 286 (2022): 131913. https://doi.org/10.1016/j.chemosphere.2021.131913

[31] Mansir, Nasar, Yun Hin Taufiq-Yap, Umer Rashid, and Ibrahim M. Lokman. "Investigation of heterogeneous solid acid catalyst performance on low grade feedstocks for biodiesel production: A review." *Energy Conversion and Management* 141 (2017): 171-182. https://doi.org/10.1016/j.enconman.2016.07.037

[32] Kamaldin, Nurul Nadirah Mohd, Muzakkir Mohammad Zainol, Nurin Qistina Saperi, Abdull Hafidz Hassan, Kamrul Ridwan Zainuddin, Mohd Asmadi, Nour Sariyan Suhaimin, and Nor Aishah Saidina Amin. "Pretreatment of Empty Fruit Bunch using Various Choline Chloride-based Acidic Deep Eutectic Solvents." *Malaysian Journal of Chemistry* 25, no. 3 (2023): 139-149. https://doi.org/10.55373/mjchem.v25i3.139

[33] Bakhtiar, M. H. A. B. M., N. B. A. Sari, A. Bin Yaacob, M. F. B. M. Yunus, and K. Bin Ismail. "Characterization of oil palm Empty Fruit Bunch (EFB) biochar activated with potassium hydroxide under different pyrolysis temperature." *Journal of Engineering Science and Technology* 14, no. 5 (2019): 2792-2807.

[34] Shohaimi, Norshahidatul Akmar Mohd, and Fatin Nur Syahirah Marodzi. "Transesterifikasi sisa minyak masak dalam pengeluaran biodiesel menggunakan CaO/Al_2O_3 mangkin heterogenus." *Malaysian Journal of Analytical Sciences* 22, no. 1 (2018): 157-165.

[35] Ouanji, Fatiha, Mohamed Kacimi, Mahfoud Ziyad, F. Puleo, and Leonarda F. Liotta. "Production of biodiesel at small-scale (10 L) for local power generation." *International Journal of Hydrogen Energy* 42, no. 13 (2017): 8914-8921. https://doi.org/10.1016/j.ijhydene.2016.06.182

[36] Ibrahim, Naeemah A., Umer Rashid, Balkis Hazmi, Bryan R. Moser, Fahad A. Alharthi, Samuel Lalthazuala Rokhum, and Chawalit Ngamcharussrivichai. "Biodiesel production from waste cooking oil using magnetic bifunctional calcium and iron oxide nanocatalysts derived from empty fruit bunch." *Fuel* 317 (2022): 123525. https://doi.org/10.1016/j.fuel.2022.123525

[37] Danish, Muhammad, Muhammad Waseem Mumtaz, Mahpara Fakhar, and Umer Rashid. "Response surface methodology based optimized purification of the residual glycerol from biodiesel production process." *Chiang Mai Journal of Science* 44, no. 4 (2017): 1570-1582.

[38] Nasir, Nurul Fitriah, M. F. Mirus, and Manal Ismail. "Purification of crude glycerol from transesterification reaction of palm oil using direct method and multistep method." In *IOP Conference Series: Materials Science and Engineering*, vol. 243, no. 1, p. 012015. IOP Publishing, 2017. https://doi.org/10.1088/1757-899X/243/1/012015

[39] Abdullah, N., F. Sulaiman, and H. Gerhauser. "Characterisation of oil palm empty fruit bunches for fuel application." *Journal of Physical Science* 22, no. 1 (2011): 1-24.

[40] Farid, Mohammed Abdillah Ahmad, Mohd Ali Hassan, Yun Hin Taufiq-Yap, Mohd Lokman Ibrahim, Mohd Ridzuan Othman, Ahmad Amiruddin Mohd Ali, and Yoshihito Shirai. "Production of methyl esters from waste cooking oil using a heterogeneous biomass-based catalyst." *Renewable Energy* 114 (2017): 638-643. https://doi.org/10.1016/j.renene.2017.07.064

[41] Maniam, G. P., N. Hindryawati, I. Nurfitri, R. Jose, M. H. A. Rahim, and M. M. Yusoff. "Ultrasound-aided in situ transesterification of oil adsorbed on decanter cake using EFBA and Na_2SiO_3 as catalysts." In *Fifth International Symposium on Energy from Biomass and Waste*, pp. 1-11. 2014.

[42] Mohiddin, Mohd Nurfirdaus Bin, Yie Hua Tan, Yee Xuan Seow, Jibrail Kansedo, N. M. Mubarak, Mohammad Omar Abdullah, Yen San Chan, and Mohammad Khalid. "Evaluation on feedstock, technologies, catalyst and reactor for sustainable biodiesel production: A review." *Journal of Industrial and Engineering Chemistry* 98 (2021): 60-81. https://doi.org/10.1016/j.jiec.2021.03.036

[43] Yaakob, Zahira, Irwan Sukma Bin Sukarman, Binitha Narayanan, Siti Rozaimah Sheikh Abdullah, and Manal Ismail. "Utilization of palm empty fruit bunch for the production of biodiesel from Jatropha curcas oil." *Bioresource Technology* 104 (2012): 695-700. https://doi.org/10.1016/j.biortech.2011.10.058

[44] Husin, H., T. M. Asnawi, A. Firdaus, H. Husaini, I. Ibrahim, and F. Hasfita. "Solid catalyst nanoparticles derived from oil-palm empty fruit bunches (OP-EFB) as a renewable catalyst for biodiesel production." In *IOP Conference Series: Materials Science and Engineering*, vol. 358, p. 012008. IOP Publishing, 2018. https://doi.org/10.1088/1757-899X/358/1/012008

[45] Lubis, Hamzah. "Renewable energy of rice husk for reducing fossil energy in Indonesia." *Journal of Advanced Research in Applied Sciences and Engineering Technology* 11, no. 1 (2018): 17-22.